Journal of the European Ceramic Society 21 (2001) 2153–2160

www.elsevier.com/locate/jeurceramsoc

The influence of green processing on the sintering and mechanical properties of β-sialon

A.A. Kudyba-Jansen [a,b], H.T. Hintzen [a,*], R. Metselaar [a]

[a] *Laboratory of Solid State and Materials Chemistry, Eindhoven University of Technology, PO Box 513, 5600 MB Eindhoven, The Netherlands*
[b] *Material Science Department, Silesian Technical University, Katowice, Krasinskiego 8B, 40-019 Katowice, Poland*

Received 26 February 2000; received in revised form 11 September 2000; accepted 11 October 2000

Abstract

The strength and structure of β-sialon ceramics prepared by slip casting with a different degree of flocculation was investigated. Commercial β-sialon ($z=0.5$) powder with 7 wt.% Y_2O_3 as sintering additive powder was used. Four different suspensions were prepared ranging from completely deflocculated to strongly flocculated. The degree of flocculation was checked with zeta potential and rheology investigations. The mechanical properties and microstructure of the green material reflected the varying degree of flocculation. After sintering, the various sintered materials showed similar mechanical properties for all ceramics. The strength was about 850 MPa, the toughness 4.4 MPa $m^{1/2}$ and hardness about 15.8 GPa. Accordingly the different green products were homogenised during sintering. This occurred even for samples with very low green density thanks to the favourable powder characteristics (shape, distribution, chemical composition) and liquid phase sintering with sufficient amount of sintering additive.

Keywords: Flocculation; Mechanical properties; Sialons; Sintering; Slip casting

1. Introduction

β-Sialon ceramics find applications as high temperature, corrosion resistant, thermal shock resistant, high strength and toughness structural ceramics.[1–3] Near net shaping processing is required in order to avoid machining and reduce costs. Slip casting has been reported as a suitable, inexpensive consolidation process to produce materials with high green densities and homogeneity of microstructure, even for complex geometries.[4–6,38–41]

For alumina, as it has been reported, the flocculation degree of the suspension influences both the consolidation properties and the final porosities.[7–9] For Si_3N_4 the information is often contradictory. Olagnon et al.[10] investigated the influence of Si_3N_4 slip properties and powder milling on sintering and mechanical properties. They concluded that there is no correlation between green density and final sintered density, and that the particle size distribution of the powder was the most important parameter for the final density. Pugh et al.[11] also found that density variations are removed with liquid phase sintering. They conclude from fracture studies that mechanical properties are determined by microstructural inhomogeneities such as large pores or low density regions rather than machining flaws. Sanders et al.[12] on the other hand find an influence of the milling time, which can be attributed to agglomerate size distribution. Summarising one can say that powder characteristics,[7–11] suspension behaviour[6,13–15] and sintering[16–19] influence the final product properties.

This paper reports the investigation of the influence of the suspension flocculation degree and the particle size distribution on both the green product and the mechanical properties of sintered sialon ceramics.

2. Experimental procedure

2.1. Suspension preparation and characterisation

The used powder was β-sialon, $Si_{6-z}Al_zO_zN_{8-z}$ ($z=0.5$) mixed with 7 wt.% Y_2O_3 (Syalon 101, Lukas Cookson, UK). The powder has spherical particles, a

* Corresponding author. Tel.: +31-40-247-3113; fax: +31-40-244-5619.
E-mail address: h.t.hintzen@tue.nl (H.T. Hintzen).

0955-2219/01/$ - see front matter
PII: S0955-2219(00)00289-2

monodisperse grain size distribution with median (d_{50}) of 0.84 μm, mean 0.64 μm and specific surface area of 9.4 m^2/g.

The powder was suspended in water and 0.3 wt.% of the ammonium polyacrylate surfactant, Dolapix CE64 Zschimmer & Schwarz, was added.[20] The suspension was prepared by mixing the powder with demineralised water in a plastic bottle with Si_3N_4 milling balls on a roller bench for 24 h. The resulting suspensions, with a solid loading of 42 wt.%, were sieved over a screen with openings of 33 μm. The pH was adjusted using 0.1 and 0.4 M HNO_3 or 0.1 M NH_4OH and the suspensions were subsequently left for 24 h on a roller bench.

The zeta potential of the suspensions was measured using the DELSA 440 system and Zeta Sizer 4 (Model AZ 6004, Malvern Instruments, UK) based on quasi-elastic light scattering and ZetaPals based on phase analysis light scattering in order to insure reliable zeta potential values. The rheological measurements were performed using a TA Instruments Weissenberg Rheogoniometer, fitted with a Mooney geometry (combined concentric cylinder and a cone/plate). The measurements were performed at 20°C at shear rates of 1–200 s^{-1}. The data were also analysed by TA Instruments rheology solution software. The viscosities were also calculated at a single point at a shear rate of 100 s^{-1}.

From a measurement of the zeta potential of β-sialon with 7 wt.% Y_2O_3 and 0.3 wt.% Dolapix as a function of pH we found the isoelectric point of the suspension at pH = 3.9. On the basis of analysis of zeta potential values as well as viscosity behaviour of suspensions as a function of pH, four slips were prepared with different flocculation degree. The parameters of the suspensions are given in Table 1. With increasing pH the absolute zeta potential value increases and viscosity decreases indicating decrease of flocculation degree in suspension. The suspension of pH 10.3 is completely deflocculated, while the one with pH 9.6 is slightly under deflocculated. Both are easily slip cast. The suspension with pH 6.6 is strongly flocculated and thick, the one with pH 8.6 is flocculated and has somewhat too high viscosity for slip casting.

Table 1
Parameters of the suspension of β-sialon, 7 wt.% Y_2O_3 and 0.3 wt.% dispersant

pH	Zeta (mV)	Viscosity at 100 s^{-1} (Pa·s)	Flocculation degree
6.6	−12	0.06 Shear thinning with yield	Strongly flocculated
8.6	−20	0.02 Shear thinning	Flocculated
9.6	−32	1.5×10^{-3} Newtonian	Almost deflocculated
10.3	−39	2.7×10^{-3} Newtonian	Completely deflocculated

2.2. Green product preparation and characterisation

After de-airing, the suspensions were slip cast on plaster of Paris moulds in order to form discs (diameter ≈40 mm, thickness ≈3 mm). Afterwards the green products were dried at room temperature, at 40 and at 100°C at each temperature for 24 h. Subsequently, the density was determined by weight/volume measurements.

The mechanical properties of the green samples were measured on about 10 as prepared samples per batch. The strength on green samples was measured with ring on ring (ROR) tests (17 and 30 mm rings) at room temperature and was calculated using:[21]

$$\sigma_{\mathrm{ROR}} = \frac{3(1+\nu)F}{4\pi t^2}\left\{1 + 2\ln\left(\frac{R_0}{R_i}\right) + \left(\frac{1-\nu}{1+\nu}\right)\left(\frac{R_0}{R}\right)^2\left[\frac{1}{2} - \frac{1}{2}\left(\frac{R_i}{R_0}\right)^2\right]\right\}$$

where σ_{ROR} is the strength, π is a constant, ν is the Poisson's ratio (assumed to be 0.3[22]), R the specimen radius, R_0 the ball bearing support, R_i the radius of inner support ring, F the force and t the specimen thickness. The cross-head speed used was 1 mm/min.

2.3. Ceramics preparation and characterisation

Dilatometry was performed using a gas pressure sintering furnace (KCE, Germany) with a nitrogen pressure of 10^5 Pa up to 1700°C. For the sintering a nitriding furnace (KCE, Germany) was used with a nitrogen pressure of 10^5 Pa at 1660°C for 2.5 h with a heating/cooling rate of 10°C/min. For the sintering, the samples were embedded in a powder bed consisting of β-sialon with Y_2O_3, Si_3N_4 and BN inside a BN crucible.

In order to perform mechanical tests all samples were carefully ground to 1 mm thickness. The samples were ground with a diamond wheel (D46 i.e. average grain size of diamond 46 μm) removing 3 μm per step and the last 20 μm removing 0.5 μm per step. Subsequently, they were ground with SiC abrasive paper of 800 mesh. Afterwards a few samples were polished for microstructural analysis and density measurements applying the Archimedes method in water.

The microstructure studies of green and sintered products were done using scanning electron microscopy (SEM Jeol 840). The element analysis was performed with electron probe microanalysis (EPMA with Jeol JXA-8600SX) using wavelength dispersive spectrometry (WDS). SEM image processing allowed estimation of porosity and Y_2O_3 distribution and content in the ceramics. Optical microscopy was used for macroscopic porosity observations.

The mechanical properties of ceramics were measured on 20 ground samples per batch. The strength of ceramics was measured using ball on ring (BOR) (12 mm ring) tests and calaculated with the equation:[23]

$$\sigma_{BOR} = \frac{3(1+\nu)F}{4\pi t^2}\left\{1 + 2\ln\left(\frac{R_0}{b}\right) + \left(\frac{1-\nu}{1+\nu}\right)\left(\frac{R_0}{R}\right)^2\left[1 - \left(\frac{b}{R_0}\right)^2\right]\right\}$$

where σ_{BOR} is the strength, π is a constant, ν is the Poisson's ratio (assumed to be 0.3[22]), R the specimen radius, R_0 the ball bearing support, b the contact radius loading area, F is the force, and t the specimen thickness. The $b = t/3$ (Westergaard approximation) was used. The cross-head speed used was 1 mm/min.

The Weibull modulus, m, was calculated by least squares fitting the strength versus $P_{fi} = (i-0.5)/n$, where P_{fi} is the probability of the ith ranked specimen and n the total number of specimens used.

The hardness was measured using a Vickers indenter applying 4.9, 9.81, 19.61 and 156.3 N loads and was calculated using the equation

$$H_V = 1.890 \cdot \frac{F}{a^2}$$

where H_V (GPa) is the Vickers hardness, F is force (N) and a is the indent diameter (μm).

The load independent hardness (H_0) was calculated using the approximation of Bull et al.:[24]

$$H_0 = \frac{H_V}{\left(1 + \frac{\delta}{a}\right)^2}$$

where H_V is the measured hardness (GPa), a is the indent diameter (μm) and δ is the amount of elastic recovery (μm). The elastic recovery was calculated by fitting the measured data for different loads applied.

The fracture toughness was calculated from the (Vicker's) hardness measurement using[25]

$$K_{Ic} = 0.016 \frac{\sqrt{\left(\frac{E}{H_V}\right)} \cdot F}{c^{\frac{3}{2}}}$$

where K_{Ic} is the fracture toughness (MPa $m^{1/2}$), E is the Young's modulus (avg. 240 GPa[26]), H_V is the Vickers hardness (GPa), c is the crack length (μm) and F is the applied load, 156.3 N.

Since in the BOR test a large gradient of the stress field exists and a simple estimate of the flaw size requires a more or less uniform stress field, it seems more appropriate to use the stress that would be present in a 4 point bending test (σ_{4pb}). To this purpose we use a correction factor of 0.83. The flaw size is estimated as

$$a = \left(\frac{K_{Ic}}{Y \cdot \sigma_{4pb}}\right)^2$$

where a is a defect size (μm), Y is the shape factor (−) taken as 1.26 appropriate for hemi-spherical surface defects and σ_{4pb} is the calculated 4 point bending strength (MPa).

The thermal diffusivity was measured on polished discs coated on one side with carbon using photo flash equipment (Compotherm Messtechnik GmbH). Using vacuum during measurements the convective losses were minimised. The thermal conductivity was calculated using:

$$\kappa = \rho \cdot c_v \cdot a \ [\mathrm{W\ m^{-1}\ K^{-1}}]$$

where ρ is the density (mol m^{-3}), c_v the specific heat (J K^{-1} mol^{-1}) and a the thermal diffusivity (m^2 s^{-1}). In the absence of the specific heat of sialon we used the value for Si_3N_4 (99.533 J K^{-1} mol^{-1}).[27]

3. Results and discussion

3.1. Green product preparation and characterisation

Fig. 1 shows the effect of flocculation (= pH) on cake growth of the cast suspensions as a function of time. All curves show parabolic cake growth. The rate constant, k, from the growth equation

$$d = k \cdot t^{1/2}$$

where d is the cake thickness at time t, is given in Table 2. For the suspension of pH 9.6 the cake formation was slowest while the highest green density was obtained. The suspensions of pH 10.3 and 8.6 resulted in a similar green density, although they had different casting rates. The change of slope obtained at pH 8.6 is due to ageing of the suspension during slip casting and the accompanying sedimentation. The suspension of pH 6.6 formed the cake at once, what resulted in the lowest cake density. The density of the different cakes are given in Table 2.

Apart from the densities also the microstructures of the green products were different. The most homogeneous packing of the green product was observed for the top layer of the pH 9.6 suspension (Fig. 2a). This whole sample, including the bottom (Fig. 2b), was the most uniform from all of the investigated samples. The strongest agglomeration, as could be expected, was found in sample pH 6.6 (Fig. 3).

The influence of the flocculation degree on the strength and Weibull moduli of the green samples is also given in Table 2. The highest strength and Weibull modulus were obtained for samples almost (pH 9.6) and completely deflocculated (pH 10.3). For the remaining green samples the values decreased with the decreasing deflocculation degree. The almost completely deflocculated

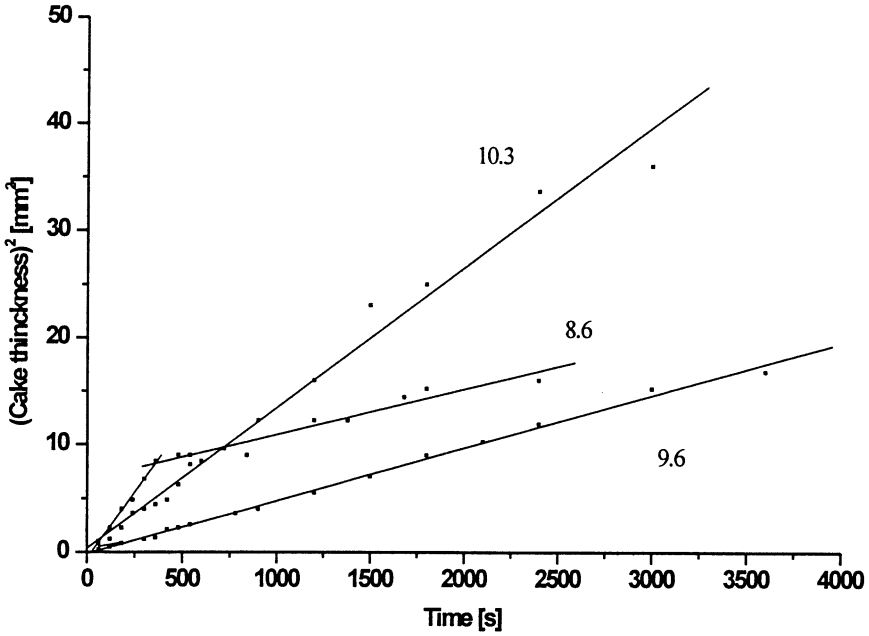

Fig. 1. Effect of pH (flocculation degree) on cake growth as a function of time.

Table 2
Characteristics of the sialon cake formation and green products

Sample code	1	2	3	4
pH of suspension	6.6	8.6	9.6	10.3
Casting rate constant (mm/min$^{1/2}$)	Instant formation	0.024	0.005	0.014
Green density (g/cm^3)	1.3	1.51	1.9	1.55
Relative density (% TD)	40	46	59	46
Remarks	Instant cake formation	Chipping off	Strong	Fragile
ROR strength (MPa)	0.3	0.6	0.78	0.73
Weibull modulus	2.2	3.3	5.2	4.5

suspension (pH 9.6) resulted in the strongest sample and most uniform green product.

3.2. Ceramics preparation and characterisation

Typical dilatometer shrinkage and shrinkage rate curves are shown in Fig. 4. The curves agree quite well with those from earlier publications on liquid phase sintering of sialons.[28,29] The high peak at about 1500°C is attributed to pore elimination by particle rearrangement and co-operative flow of the particle/liquid mixture in the solution-reprecipitation stage. The second small maximum at about 1700°C is attributed to grain growth.[30] As shown in Table 3 the relative densities of the samples after sintering are in all cases 99%, in spite of the differences in green densities. If we compare this behaviour with literature data on solid state sintering we note a remarkable difference. In that case the green structure can be found back in the sintered product. We conclude from this that the liquid phase sintering has a curing effect on defects in the green product. Of course tablets from the four batches showed significant differences in shrinkage in diameter and thickness depending on the green density. This means that, although a high sintered density can be obtained, independent of the green density, the large shrinkage can be detrimental in case of ceramic products with more complex shapes.

For all four batches, the sintering resulted in a uniform, needle-like microstructure, characteristic for β-sialon with a liquid phase containing yttria, (white phase in between grains) (Fig. 5). The element mapping (EPMA) revealed a uniform distribution of Si, Al, N, O and Y. Sporadically on an yttrium map a higher intensity spot has been found indicating a larger concentration of liquid phase between the grains.

A polished cross-section of the raw samples revealed some porosity as observed with SEM and optical microscopy. The observed porosity is slightly exaggerated due to breaking out of pieces during polishing. The porosity distribution visible on the cross-section of the raw samples seems to be the only reminiscence of the flocculation degree. Analysis of the SEM and optical

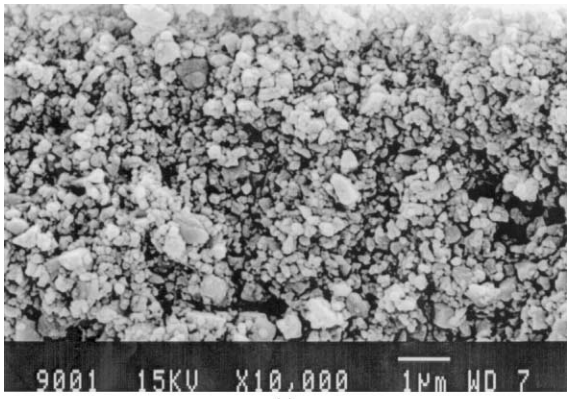

(a)

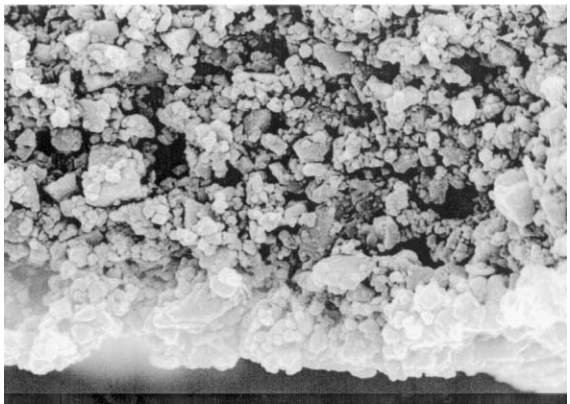

(b)

Fig. 2. Cross-sections of the green sample 3, prepared at pH 9.6. (a) Top layer. (b) Bottom layer.

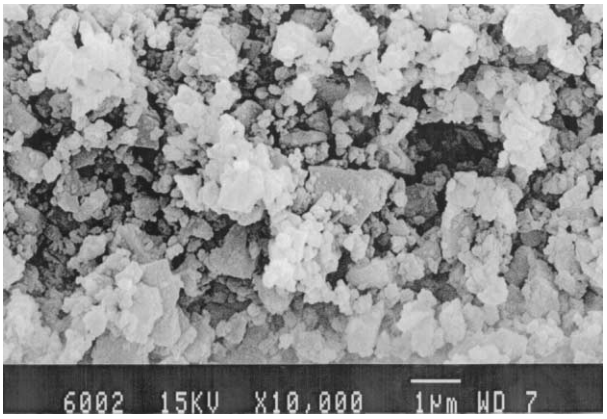

Fig. 3. Bottom layer of the cross-section of the green sample 1, prepared at pH 6.6.

microscope images (Figs. 6 and 7) showed that the pH 9.6 sample has the most uniform porosity distribution (Fig. 6), while the other samples show significantly less porosity at the bottom and varying distribution throughout the rest of the sample. The porosity distribution of samples of pH 10.3 and pH 9.6 is shown in

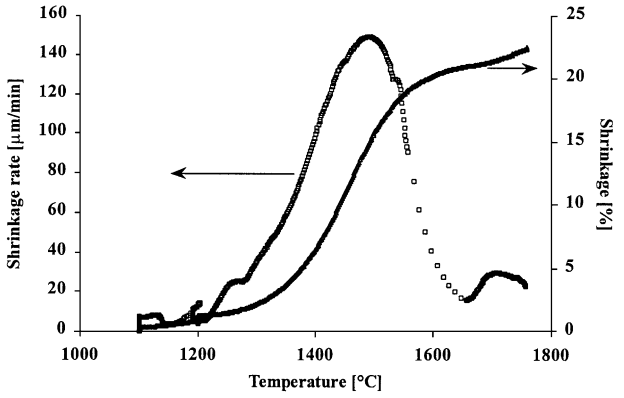

Fig. 4. Dilatometer shrinkage curves of β-sialon.

Table 3
Characteristics of sialon green and sintered samples

Sample code	1	2	3	4
pH of suspension	6.6	8.6	9.6	10.3
Green density (% TD)	40	46	59	46
Sintered density (% TD)	98.9	99.1	99.0	98.8
BOR (MPa)	880	840	880	770
4pt bending[a] (MPa)	730	700	730	640
Weibull modulus	9	10	10	10
Vickers hardness H_0 (GPa)	15.6	15.8	15.8	16.8
Elastic recovery δ	2.7	2.4	2.8	2.3
K_{Ic} (MPa $m^{1/2}$)	4.6	4.7	4.7	4.3
Thermal conductivity (W/mK)	24	25	21	24

[a] Calculated from BOR by $\sigma(4pt) = 0.83 \cdot \sigma$ (BOR).

Figs. 6 and 7. The lower porosity at the bottom of the samples is due to high suction pressure and liquid pressure at the beginning of slip casting. Later during slip casting and liquid removal the flocculated structure can be better preserved resulting in higher porosity. From the optical micrographs we observe the lowest overall porosity in sample 3, prepared at pH = 9.6, followed by those prepared at pH 10.3, 8.6 and 6.6.

3.2.1. Thermal properties of ceramics

Since only few data are available of the thermal properties of sialon we measured the diffusivity of our samples and from these data the thermal conductivities were calculated (Table 3). Mitomo et al.[31] measured thermal conductivities of β-sialon as a function of the z-value and found a linear relationship between the thermal resisitivity and z. Because of the increased impurity scattering with increasing z value, a rapid decrease of κ is observed. Our value of 25 W/mK for $z = 0.5$ is somewhat higher than the value of 19 W/mK reported by Mitomo et al.,[31] which shows that there is less phonon scattering in our samples. It is seen from Table 3 that the conductivity values show no clear relation with the preparation conditions.

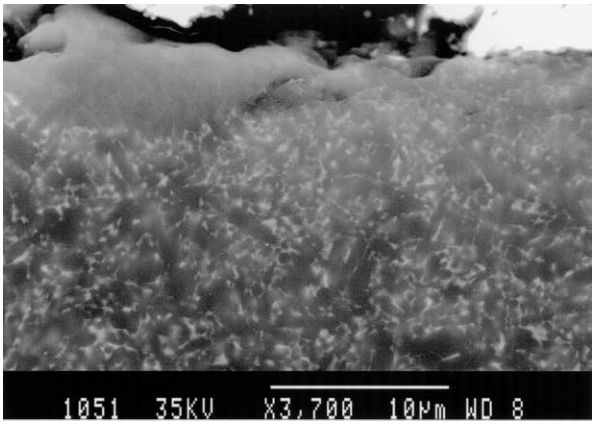

Fig. 5. Microstructure of a sintered sample (cross-section).

3.2.2. Mechanical properties of ceramics

The hardness decreases with increasing load for all samples. The decrease is caused by elastic recovery of material when the applied load is removed and is called the indentation effect. In order to account for this effect the method of Bull et al.[24] was applied. The load independent hardness, H_0, and the elastic recovery, δ, of the β-sialon ceramics produced from the suspensions of different pH's are presented in Table 3. It is clear that the load independent hardness is the same for all the samples. The different flocculation degrees did not influence the hardness of the sintered samples.

Table 3 also shows values for the fracture toughness and strength. As can be observed these values are almost the same for all samples. Only sample 4, prepared at pH 10.3 showed slightly lower values. From the fracture toughness and strength the defect size was calculated to be about 28 μm for all samples.

Investigations of the fracture surfaces revealed that the fracture occurred not in the centre but on the side of the samples and on the surface in a polishing groove. This implied that the grinding was responsible for the failure of the ceramic discs and that internal defects are smaller than machining defects. This shows once more that the structure was homogenised and possible internal defects were cured during sintering.

Volume defects of 24–40 μm in size were reported to be the cause of the failure in previous studies of β-sialon ceramics.[26] In the work of Van der Heijde et al.,[26] a carbothermally produced powder was used. Their powder was attrition milled, had a relatively wide size distribution as compared to commercial powders, and the particles were not spherical. The powder characteristics could be the origin of the failure of the ceramics at volume defects. The strength of our sialon with $z=0.5$ corresponds well with values of 560 and 610 MPa reported in literature.[32,33] It is generally observed that the strength of the β-sialon ceramics with $z=3$ is less than β-sialon ceramics with lower z value.

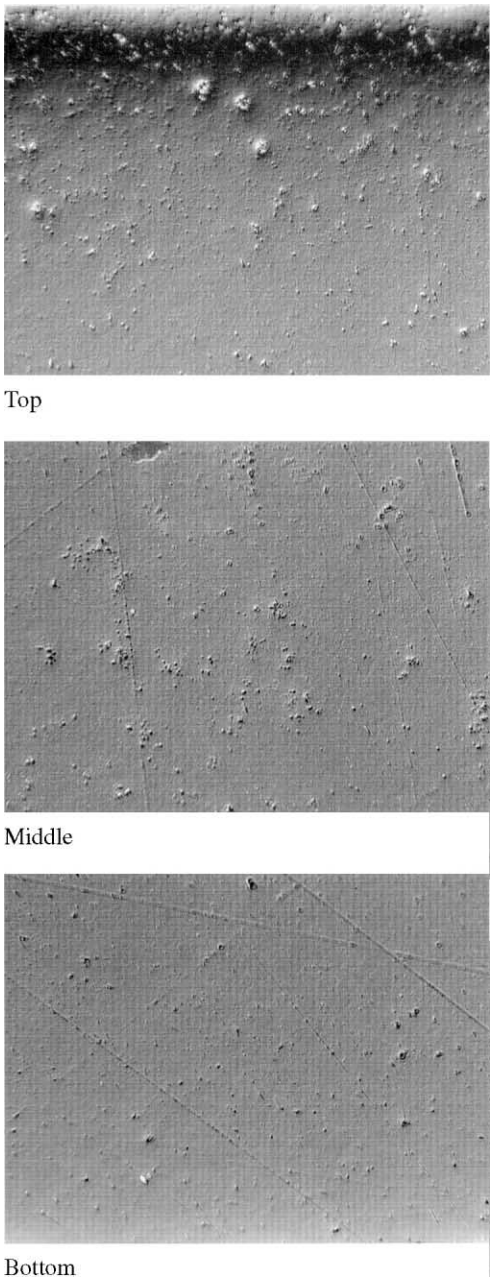

Fig. 6. Porosity distribution observed on the cross-section of the sintered sample 4, prepared at pH 10.3 under an optical microscope.

Since data on the influence of the processing of sialon on the mechanical properties are scarce, a comparison with Si_3N_4 is opportune. For instance, Kamiya et al.[34] concluded that the specific surface area of a fine powder and the average pore size or distance between the particles in a green compact determined the relative density of Si_3N_4 sintered bodies. They postulated that if the pore size is too large the improvement of the structure and reaching a full density is impossible. Shaw[35] also found that pore size distribution is crucial for the densification, which is driven by capillary forces. If there is a strongly bimodal distribution of pores the densification

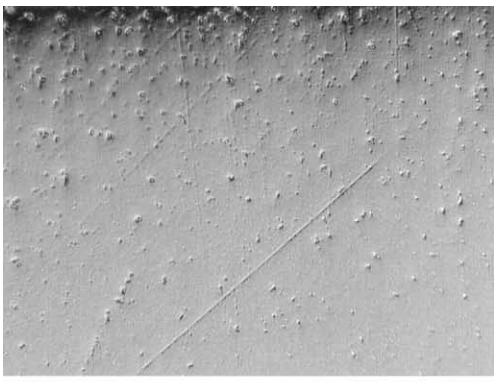

Fig. 7. Porosity distribution observed on the cross-section of the sintered sample 3, prepared at pH 9.6 under an optical microscope.

rate may change abruptly and the large pores will not disappear leaving less dense and weaker product. As well as Shaw, Schmidt et al.[36] claim that the capillary forces at elevated sintering temperatures are responsible for a homogenous distribution of the liquid throughout the sample and hence, compensate initial inhomogeneities in sintering aid distribution. According to Yang et al.[37] a homogenous distribution of sintering additive improved the sinterability due to increased reactivity, what resulted in a denser and more homogenous product.

In this respect, we can conclude that a fine powder with high activity formed into a green compact with a narrow pore size distribution, though not necessarily high density, with a uniformly distributed sintering additive will result in a dense homogenous sintered product.

This agrees with the conclusion from this work that the flocculation degree does not significantly influence the mechanical properties. It is concluded that with the present powder characteristics, a sufficient amount of liquid phase during the liquid phase sintering homogenises the differences in green microstructures.

4. Conclusions

Using sialon suspensions with different degrees of flocculation, green samples with significantly different relative densities were obtained. However, this did not influence the relative densities of the sintered β-sialon ceramics. All samples showed a homogenous microstructure. The obtained strength and fracture toughness values were comparable to literature data of other β-sialon ceramics obtained by optimised slip casting. The high shrinkage during sintering which occurred when flocculated sialon suspensions were used and the similarity of mechanical properties for all batches indicate that the powder characteristics and liquid phase sintering were responsible for elimination of the structural differences in green products.

Acknowledgements

Fraser McNiel-Watson, Brookhaven Instruments Corporation, USA, is acknowledged for the zeta potential measurements. Prof. G. de With and Dr. L.J.M.G. Dortmans are acknowledged for their help and expertise.

References

1. Ekström, T. and Nygren, M., SiAlON ceramics. *J. Am. Ceram. Soc.*, 1992, **75**, 259.
2. Cother, N. E. and Hodgson, P., The development of Sylon ceramics and their engineering applications. *Trans. J. Br. Ceram. Soc.*, 1982, **81**, 141.
3. Arato, P., Besenyei, E., Kele, A. and Weber, F., Mechanical characteristics and application of syalon ceramics. *TIZ intern. Powder Magazine*, **9**, 1989.
4. Oda, K., Mizuta, H., Shibasaki, Y. and Ohshima, K., Slip casting of silicon nitride and mechanical properties of sintered bodies (Part 1). *J. Ceram. Soc. Jap*, 1992, **100**, 708.
5. Castanho, S. M. and Moreno, R., Rheological properties of silicon nitride aqueous casting slips. In *Third Euro-Ceramics*, Vol. 1. ed. P. Duran and J. F. Fernandez. Faenza Edritice Iberica, Castellon de la Plana, 1993, p. 513.
6. Albano, M. P. and Garrido, L. B., Processing of concentrated aqueous silicon nitride slips by slip casting. *J. Am. Ceram. Soc.*, 1998, **81**, 837.

7. Bergström, L., Schilling, C. and Aksay, I. A., Consolidation behaviour of flocculated alumina suspensions. *J. Am. Ceram. Soc.*, 1992, **75**, 3305.
8. Lange, F. F., powder processing science and technology for increased reliability. *J. Am. Ceram. Soc.*, 1989, **72**, 3.
9. Lamas, A. G., Almeida, M. and Diz, H. M. M., Slip casting of alumina bodies with differential porosities. *Ceramics International*, 1993, **19**, 121.
10. Olagnon, C., McGarry, D. and Nagy, E., The effect of slip casting parameters on the sintering and final properties of Si_3N_4. *Br. Ceram. Trans. J.*, 1989, **88**, 75.
11. Pugh, M.D. and Drew, R.A.L., Processing improvements in a sintered Si_3N_4 material. *Ceramics Materials and Components for Engines*, *Proceedings 3rd Symposium*, Las Vegas, 1988. p. 139.
12. Sanders, W. A., Kiser, J. D. and Freedman, M. R., Slurry processing consolidation of silicon nitride. *Am. Ceram. Soc. Bull*, 1989, **68**, 1836.
13. Bergström, L. and Shinozaki, K., Effect of interactions on the colloidal properties and packing of nanosized powders. In *Fourth Euro Ceramics*, Vol. 2. ed. C. Galassi. Gruppo Editoriale Faenza Editrice S.p.A., Italy, 1995, pp. 3–14.
14. Nunes, F., Lamas, A. G., Almeida, M. and Diz, H. M. M., Influence of deflocculants on the characterristics of alumina bodies obtained by slip casting. *J. Mater. Sci.*, 1992, **27**, 6662.
15. Tsudo, H., Sashida, N., Yamakawa, T. and Miyata, N., Slip casting of sialon for pressureless sintering. *J. Mater. Sci.*, 1998, **33**, 2889.
16. Arato, P., Besenyei, E., Kele, A. and Weber, F., Effect of sintering parameters on microstructure and properties of sialon materials. In *VII World Round Table Conference on Sintering*, Hercegovina, 1989. Plenum Press, 1990.
17. Kokmeijer, E., Scholte, C., Blömer, F. and Metselaar, R., The influence of process parameters and starting composition on the carbothermal production of sialon. *J. Mater. Sci.*, 1990, **25**, 1261.
18. Ekström, T. and Ingelström, N., Characterisation and properties of sialon materials. In *Non Oxide Technical and Engineering Ceramics*, ed. S. Hampshire. Elsevier Applied Science, London, 1986, p. 231.
19. Kokmeijer, E., de With, G. and Metselaar, R., Microstructure and Mechanical Properties of β-sialon ceramics. *J. Eur. Ceram. Soc.*, 1991, **8**, 71.
20. Kudyba-Jansen, A., Almeida, M., van der Heijde, J. C. T., Lavèn, J., Hintzen, H. T. and Metselaar, R., Aqueous processing of carbothermally prepared Ca-α-SiAlON and β-SiAlON powders: powders and suspension characterisation. *J. Eur. Cer. Soc.*, 1999, **19**, 2711.
21. Scholten, H. F., Dortmans, L., de With, G., de Smet, B. and Bach, P., *J. Eur. Ceram. Soc.*, 1992, **10**, 33.
22. Dijen van, F. K., The carbothermal production of $Si_3Al_3O_3N_5$ from kaolin, its sintering and its properties. Ph.D. Thesis Eindhoven University of Technology, 1986.
23. With de, G. and Wagemans, H. H. M., Ball on ring test revisited. *J. Am. Ceram. Soc.*, 1989, **72**(8), 1538.
24. Bull, S. J., Page, T. F. and Yoffe, E. H., An explanation of the indentation size effect in ceramics. *Philosophical Magazine Letters*, 1989, **59**, 281.
25. Liang, K. M., Orange, G. and Fantozzi, G., Evaluation by indentation of fracture toughness of ceramic materials. *J. Mater. Sci.*, 1990, **25**, 207.
26. Heijde van der, J. C. T., Terpstra, R. A., van Rutten, J. W. T. and Metselaar, R., Total aqueous processing of carbothermal produced β-SiAlON. *J. Eur. Ceram. Soc.*, 1996, **17**, 319.
27. Chase, M.W., et.al., JANAF thermochemical tables third edition, Part I, Al-Co. *Journal of Physical and Chemical Referenca Data*, 1985, **14.**
28. Cao, G. Z. and Metselaar, R., α′-Sialon ceramics: a review. *Chem. Mater.*, 1991, **3**, 242.
29. Watari, K., Nagaoka, T. and Kanzaki, S., Densification process of α-sialon ceramics. *J. Mat. Sci.*, 1994, **29**, 5801.
30. Cao, G. Z., Metselaar, R. and Ziegler, G., Relations between composition and microstructure of sialons. *J. Eur. Ceram. Soc.*, 1993, **11**, 115.
31. Mitomo, M., Hirosaki, N. and Mitsuhashi, T., Thermal conductivity of α-sialons. *J. Mater. Sci. Letters*, 1984, **3**, 915.
32. Suzuki, S., Nasu, T., Hayama, S. and Ozawa, M., Mechanical and thermal properties of β-sialon prepared by a slip casting method. *J. Am. Ceram. Soc.*, 1996, **79**, 1685.
33. Hayama, S., Takakuni, N., Ozawa, M. and Suzuki, S., Mechanical properties and microstructure of reaction sintered β-sialon ceramics prepared by slip casting method. *J. Mater. Sci.*, 1997, **32**, 4973.
34. Kamiya, H., Isomura, K., Jimbo, G., Hotta, T. and Tsubaki, J., Influence of powder properties and green microstructure on the sintering behaviour of Si_3N_4. *Journal of Ceramic Society of Japan*, 1993, **101**, 277.
35. Shaw, T. M., Model for the effect of powder packing on the driving force for liquid phase sintering. *J. Am. Ceram. Soc.*, 1993, **76**(3), 664–670.
36. Schmidt, H., Oliveira, F. J., Silva, R. F. and Ferreira, J. M. F. Si_3N_4 powder doped with Y_2O_3 by organometallic compound and metal oxide: a comparative study, Developments in processing of the advanced ceramics. In *Fourth Euro Ceramics, part II*, 1995, p. 205.
37. Yang, J., Kleebe, H.-J., Martin, B. and Ziegler, G., Pressureless sinterablility of slip cast silicon nitride bodies prepared from coprecipitation-coated powders. *J. Eur. Ceram. Soc.*, 1999, **19**, 433.
38. Ohshima, K., Oda, K. and Shibasaki, Y., Slip casting of silicon nitride and mechanical properties of sintered bodies (Part 2). *J. Ceram. Soc. Jap*, 1992, **100**, 1017.
39. Ohshima, K., Oda, K., Sano, S. and Shibasaki, Y., Slip casting of Silicon Nitride and Mechanical Properties of Sintered Bodies (Part 3). *J. Ceram. Soc. Jap*, 1993, **101**, 405.
40. Sano, S., Ohshima, K., Oda, K. and Shibasaki, Y., Slip casting of Silicon Nitride and Mechanical Properties of Sintered Bodies (Part 4). *J. Ceram. Soc. Jap*, 1993, **101**, 916.
41. Sano, S., Oda, K., Ohshima, K. and Shibasaki, Y., Slip casting of silicon nitride and mechanical properties of sintered bodies (Part 5). *J. Ceram. Soc. Jap.*, 1993, **103**, 927.